

Chapter 3

Tsunami Inundation Modeling of the 2011 Tohoku Earthquake Using Three-Dimensional Building Data for Sendai, Miyagi Prefecture, Japan

Toshitaka Baba, Narumi Takahashi, Yoshiyuki Kaneda, Yasuyuki Inazawa,
and Mariko Kikkojin

Abstract In conventional modeling of tsunami inundation, based on nonlinear shallow water theory in a finite-difference scheme, the effect of buildings and structures is represented by a bottom friction parameter rather than by three-dimensional (3D) building shapes. But large, strong buildings should offer direct protection against an incoming tsunami, like seawalls. In this study, therefore, we incorporated 3D building data obtained from lidar measurements in modeling the tsunami from the 2011 Tohoku earthquake at the port of Sendai, Miyagi Prefecture, Japan, and compared the results from conventional modeling based on a digital elevation model. In the model incorporating 3D building data, the maximum inundation height was greater than in the conventional model at the front of coastal buildings and structures and smaller behind them. High-velocity currents appeared in the corridors between these buildings, and the tsunami inundation area was smaller in the residential zone because of the obstacles that buildings presented to the tsunami. These results mean that solid buildings and structures have a significant influence on the propagation of tsunamis on land. The effects of the 3D shapes of buildings and structures should be further investigated for detailed tsunami hazard assessments in urban areas.

Keywords 2011 Tohoku Tsunami • Tsunami modeling • 3D Building data

T. Baba (✉) • N. Takahashi • Y. Kaneda

Japan Agency for Marine-Earth Science and Technology (JAMSTEC), Yokohama
Institute for Earth Sciences, 3173-25 Showa-machi, Kanazawa-ku, Yokohama,
Kanagawa 236-0001, Japan
e-mail: babat@jamstec.go.jp

Y. Inazawa • M. Kikkojin

Geospatial Information Authority of Japan (GSI), 1 Kitasato,
Tsukuba, Ibaraki 305-0811, Japan

3.1 Introduction

The 2011 Tohoku earthquake (M 9.0) occurred on 11 March near the Japan Trench, where the Pacific plate subducts westward with respect to the North America plate at a rate of approximately 8–9 cm/year (DeMets et al. 2010). Finite fault models of this earthquake have been proposed based on seismic wave data (e.g., Ammon et al. 2011; Yagi and Fukahata 2011), crustal displacement data (e.g., Suito et al. 2011; Ito et al. 2011), and tsunami data (e.g., Satake et al. 2013). The dimensions of the rupture zone have been estimated to be about 400×200 km, and the largest slip appears to have exceeded 30 m on the plate interface, although there is some disagreement among fault models. It was the fourth greatest earthquake in the world during the last century, and it caused catastrophic damage in Japan. The Pacific coast of northeastern Japan was widely and deeply inundated by the tsunami. The Japan Meteorological Agency (JMA) immediately issued early tsunami warnings that prompted residents living in the tsunami hazard area to take steps to evacuate. Although the warnings saved many lives, the earthquake and tsunami were responsible for 15,870 fatalities and 2,814 missing (National Police Agency 2012).

The first step to mitigate tsunami disasters is a tsunami hazard map, which indicates in advance the expected inundation area from various possible tsunamis. This map can be used to construct appropriate evacuation routes to elevated locations, to select locations and candidates for tsunami evacuation buildings, and to aid in estimation of human and economic losses. Construction of these maps begins with possible scenarios for generating tsunamis based on seismological, geological, and historical evidence. Next, tsunami inundation modeling is carried out based on the earthquake scenarios. Modeling usually relies on nonlinear shallow water equations along with accurate bathymetric and topographic data. Three-dimensional (3D) shapes of breakwaters and seawalls are directly incorporated in tsunami computations because of their effects on tsunami propagation, but the shapes of buildings and structures farther inland usually cannot be considered owing to limits of spatial resolution and lack of comprehensive building data. Land areas are represented instead by a bottom friction parameter, which varies in space to represent land-use types such as building lots, agricultural land, and mountainous areas.

Lidar measurements are being carried out along the Japanese coast by the Geospatial Information Authority of Japan (GSI), which collects reflections from the ground surface plus reflections from elevated surfaces such as building roofs, roads, bridges, and the tops of trees, with high spatial resolution. Large, strong buildings may be able to interact with a tsunami like a seawall rather than be subsumed in a uniform bottom friction parameter. We infer that incorporating 3D shapes of buildings and structures obtained by lidar measurements may lead to improved modeling of tsunami inundation. In this study, therefore, the 3D building data derived from lidar measurements were embedded as topographic highs in a tsunami inundation model to investigate the effect of structure shapes. This chapter presents the results obtained with and without the 3D building data. We also discuss the advantages of using 3D building data for tsunami damage mitigation.

3.2 Construction of 3D Building Data

Since the 2011 tsunami disaster, GSI has accelerated its ongoing program of airborne lidar surveys in coastal regions for disaster mitigation purposes. For compiling our 3D building data file, defined as data on ground heights of buildings and structures distributed in a gridded pattern, we used the airborne lidar data obtained by GSI.

In addition to ground surface elevations, airborne lidar provides locations of points on the tops of buildings, structures, trees, and so on in plane rectangular 3D coordinates. These points are randomly distributed in space at intervals from 1 to 2 m. The elevated objects such as buildings and trees are filtered from the original lidar data to obtain a point dataset of ground elevations, usually called a digital elevation model (DEM) (Fig. 3.1). The DEM may then be subtracted from the original lidar data to create a point dataset of the heights of objects above ground level.

This initial dataset contains all above-ground objects, including objects such as trees and bridges that do not obstruct tsunamis. To extract only buildings and structures that would affect tsunami inundation, we made use of the government's Fundamental Geospatial Data collection, which contains outlines of buildings and structures. We were able to use the four-part classification of building types (solid building, common building, solid wall-less building, and common wall-less building) to restrict ourselves to those (solid building and common building) that could provide tsunami protection. Figure 3.2 shows an example of this step in our compilation of 3D building data.

The resulting building height data were randomly distributed in the plane rectangular coordinates. We next converted this coordinate system to latitude and longitude as required by the tsunami code we used, and then sampled the points into a grid at intervals of $2/9$ arcsec, consistent with the finest grid in the tsunami simulation.

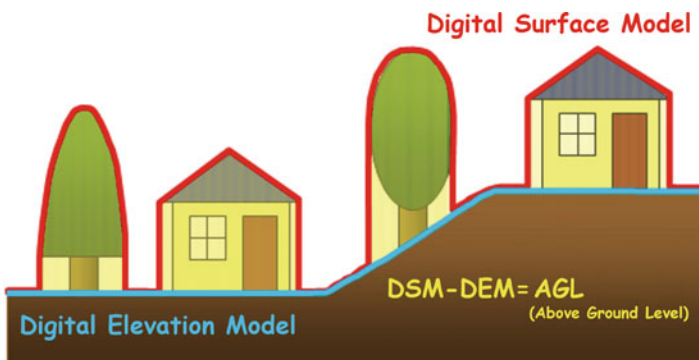


Fig. 3.1 Concepts of digital elevation model (DEM), digital surface model (DSM), and derivation of “above ground level” (AGL) data

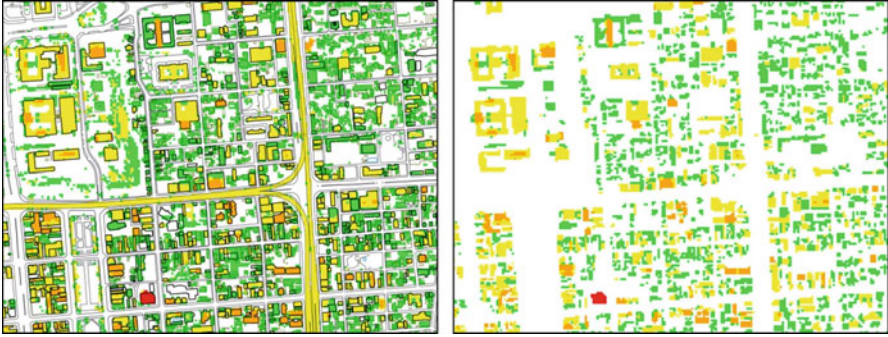


Fig. 3.2 AGL data (*left*) and 3D building data extracted from AGL data (*right*)

3.3 Tsunami Inundation Modeling

3.3.1 Computational Code and Nesting Scheme

To model the propagation and inundation of the 2011 Tohoku tsunami, we were going to use the URSGA code of Jakeman et al. (2010). This model uses a variable nested-grid scheme which allows the spatial resolution of the study region to be easily increased. It was originally based on the uniform finite-difference scheme of Satake (2002) and solves either the linear or nonlinear shallow water equations. However, a large number of grids with high spatial resolution is needed in order to assess effect of 3D shape of buildings and structures on tsunami inundation. In our case, the total number of the grids needed was going to be about 20 million. This would make the computation time too long if a serial code like URSGA is used. We therefore parallelized the URSGA code by using OpenMP and MPI in order to speed up the tsunami inundation modeling. In addition, several improvements were also made to how the nesting grids communicate. A function compatible with a GIS viewer was also developed to create snap shots of wave height distribution. Finally we also rewrote the code into Fortran90 from the original version written in C and renamed it “JAGURS”. JAGURS stands for the JAMSTEC parallelized code developed by Geoscience Australia and URS Corporation which uses Satake’s kernel. Figure 3.3 shows a result of a parallel performance evaluation test for the JAGURS. It shows that we successfully upgraded the speed of computation by the parallelizing the code.

Five nested grids as shown in Fig. 3.4 were defined for our analysis. The coarsest grid represents the entire computational domain (34–43°N, 140–147.5°E), including the tsunami source and the target area of Sendai, Miyagi Prefecture (Fig. 3.4a). The bathymetry in the grid was made using a combination of the M7000 map series provided by the Marine Information Research Center, Japan Hydrographic Association; the Tohoku bathymetric grid from JAMSTEC (Kido et al. 2011); and GEBCO data (British Oceanographic Data Centre 2010), which was interpolated

Fig. 3.3 Parallel performance test for the JAGURS code

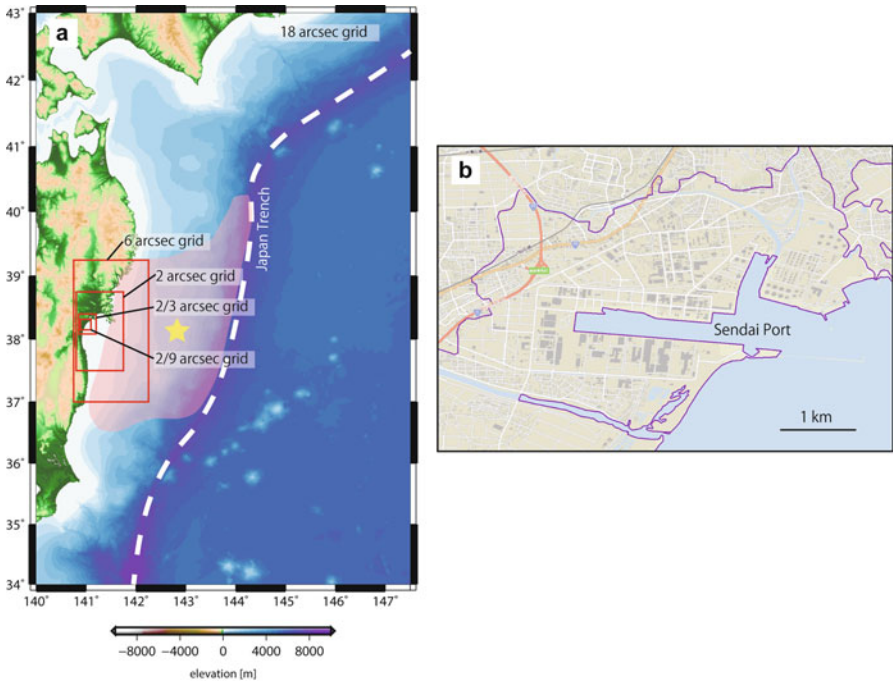
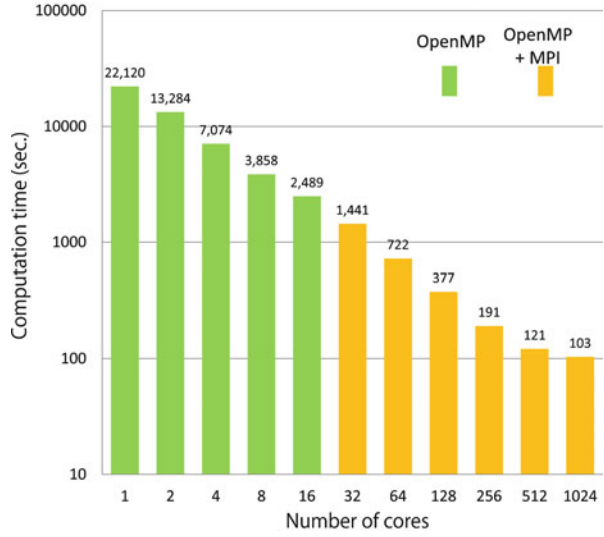


Fig. 3.4 (a) Bathymetry and topography of the computational domain (18'' grid spacing) and outlines of nested grids. *Star* indicates epicenter of the 2011 Tohoku earthquake determined by the U.S. Geological Survey. *Colored zone* is area of large slip in the fault model of Satake et al. (2013). (b) Target region of this study within the 2/9 arcsec grid. *Purple line* encloses the inundation area of the 2011 Tohoku earthquake surveyed by GSI (2011)

to 18 arcsec intervals. The M7000 series is a set of digital bathymetric contours made by combining the basic map of the coastal waters of Japan and other bathymetric information. The Tohoku bathymetric grid includes all results from JAMSTEC's multi-narrow beam surveys conducted in the Japan Trench. GEBCO provides global bathymetry datasets for the world's oceans with a spatial resolution of 30 arcsec. These datasets were also subsampled and interpolated, respectively, to make grids with spacings of 6, 2, 2/3, and 2/9 arcsec for the nesting scheme. The finest grid includes the area around the port of Sendai (Fig. 3.4b), where the inundation height was measured as 6–7 m by the Tohoku Tsunami Joint Survey Group (2011). Its spacing of 2/9 arcsec is almost equal to 5 m spacing.

For the land area, we resampled the GSI data to make topographic grids. The 50-m interval topographic data assembled by GSI covering all of Japan was used for the topography in grids of 18, 6, and 2 arcsec spacing. The 5-m interval topographic data provided by GSI was resampled and interpolated for the 2/3 arcsec and 2/9 arcsec grids. These topographic grids were mated to the bathymetric grids to yield seamless bathymetric–topographic grids for the entire region. The shape of the coastline, which is important in tsunami modeling, relied on the GSI topographic data. The shapes of tsunami defense facilities such as seawalls and breakwaters larger than 7.5 m were included as topography in the finest DEM data. The resulting grid is referred to here as the “DEM model.” The 3D building data created from the lidar data was added to the 2/9 arcsec DEM model to obtain the “incorporated model,” representing the total elevation including building and structure heights.

To assess the effect of the 3D shapes of buildings and structures on tsunami propagation, we also ran a simulation using a heterogeneous bottom friction parameter determined by land-use type using the DEM model instead of the incorporated model. We also added a function into the JAGURS to incorporate spatially heterogeneous bottom friction. For the Manning roughness, we used the segmentalized land-use data from the digital national land information website (Ministry of Land, Infrastructure, Transport and Tourism 2006). The roughness value was $0.02 \text{ s m}^{-1/3}$ in field, orchard, river, and lake areas, $0.03 \text{ s m}^{-1/3}$ in forest areas, $0.04 \text{ s m}^{-1/3}$ in residential areas, and $0.025 \text{ s m}^{-1/3}$ in other areas including the sea. However, this dataset has a relatively poor spatial resolution of 100 m. We accordingly interpolated it to fit the 2/9 arcsec ($\sim 5 \text{ m}$) grid. The poor resolution also meant that we could not resolve roads and buildings in residential areas in terms of bottom friction. For the finest grid scale, we assigned a Manning roughness of $0.04 \text{ s m}^{-1/3}$ to residential roads and buildings, and for the other four grids, we adopted a uniform value of $0.025 \text{ s m}^{-1/3}$.

3.4 Tsunami Computation and Results

Our tsunami model generates tsunamis by seafloor crustal deformation due to an earthquake. For the 2011 tsunami computation, we first calculated the crustal deformation of the fault model provided by Tohoku University (version 1.1)

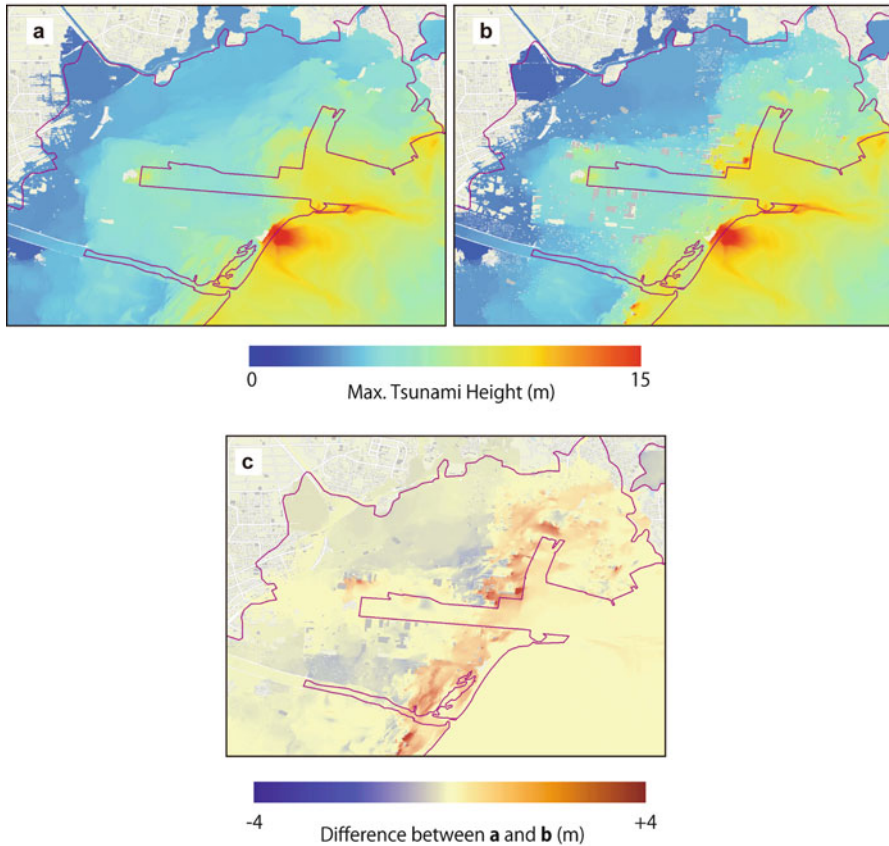


Fig. 3.5 (a) Map of maximum tsunami and inundation height computed with the DEM model. (b) Map of maximum tsunami and inundation height obtained with the incorporated model. (c) Difference between the DEM and incorporated models, with positive values indicating greater height in the incorporated model

(Imamura et al. 2011) by using the method of Okada (1985). The sea surface was deformed according to the seafloor crustal deformation with a finite rise time that was assumed to be 60 s. The topography was also modified by the same amounts at the same time. The time step used in the computation was 0.05 s in order to satisfy the stability condition of the finite difference scheme. We calculated tsunami propagation for 3 h after the Tohoku earthquake. To simulate tsunami wave propagation, we solved linear shallow water equations in the coarsest (18 arcsec) grid to save computation time and ensure stability. Nonlinear shallow water equations were applied for the four inner grids.

Figure 3.5 shows results of the tsunami analysis in the study region around Sendai. On average, the incorporated model yielded an increase in tsunami height of 2–3 m in front of coastal buildings and structures over the DEM model. For the maximum increase, the incorporated model yielded inundation heights at the front

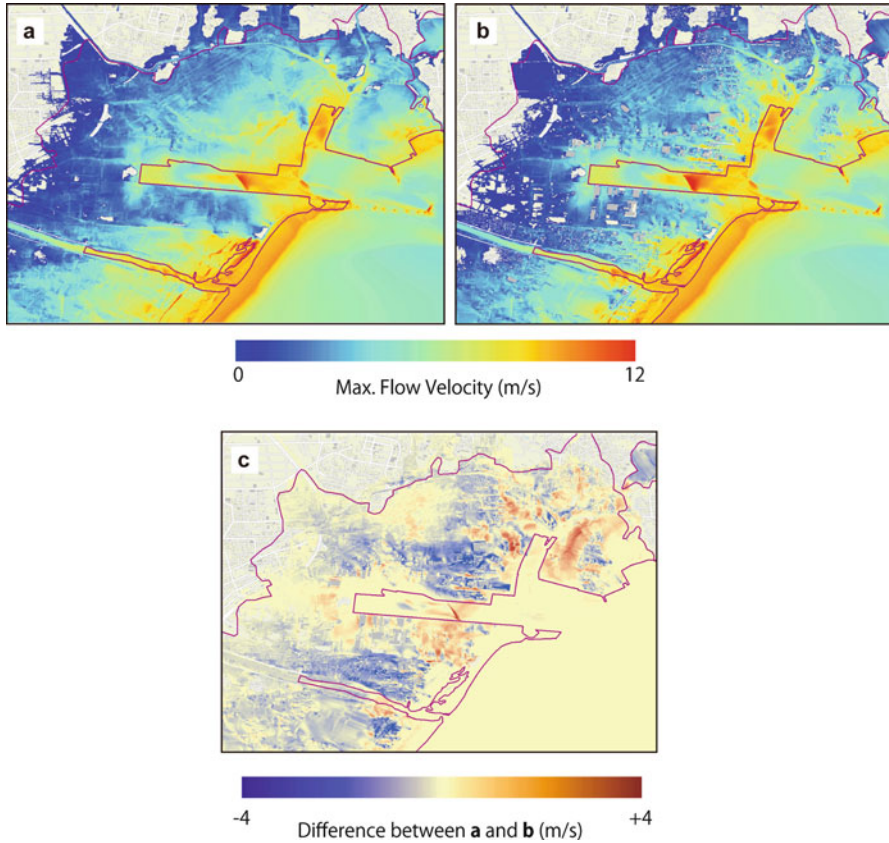


Fig. 3.6 (a) Map of maximum flow velocity computed with the DEM model. (b) Map of maximum flow velocity obtained with the incorporated model. (c) Difference between the DEM and incorporated models, with positive values indicating greater flow velocity in the incorporated model

of coastal buildings near the bay mouth that were locally as much as 9.3 m higher than those in the DEM model. But we would need detail investigations on the maximum increase of 9.3 m because the area the great increase appears is much localized. It may be an abnormal value caused by instabilities during the tsunami computation. Behind coastal buildings, inundation heights were smaller with the incorporated model than with the DEM model. The incorporated model yielded a smaller tsunami inundation area in the residential zone.

Similarly, the modeled flow velocity in the area between the buildings (Fig. 3.6) was as much as 4.75 m/s greater in the incorporated model than in the DEM model. On average, the flow velocity increased by 2–3 m/s in corridors parallel to the advance of the tsunami near the coast, a difference that gradually decreased with distance from the sea. Lower flow velocities were seen in areas directly behind buildings.

3.5 Discussion

Figures 3.5 and 3.6 show that in our simulations that incorporate the 3D shapes of buildings and structures, the tsunami height was greater in front of buildings, the flow velocity was greater in building corridors parallel to the direction of tsunami travel near the coast, and the tsunami threat was weakened behind buildings. This result indicates that buildings and structures near the coast, if they are resilient enough against the force of a tsunami, may complement seawalls and breakwaters to decrease tsunami damage in the hinterland. We conclude that incorporating 3D shapes of buildings and structures is useful in tsunami inundation modeling, especially for urban areas.

Using 3D building data in tsunami inundation modeling may also be advantageous for tsunami hazard mitigation. The tsunami hazard maps provided by the incorporated model would be useful for selecting tsunami evacuation buildings because they would account for tsunami amplification by the buildings themselves. The modeled amplification of flow in the corridors between buildings would be significant in planning tsunami evacuation routes and in planning mitigation measures to strengthen buildings. The response of residents to a tsunami may be more realistically forecasted on the basis of more accurate accounts of tsunami behavior in the urban setting. And simulations that incorporate 3D building data may be helpful in designing a tsunami resilient city in which large buildings can be designed and oriented to resist tsunami invasion into the residential hinterland.

This paper has presented the effect of using the 3D shapes of buildings and structures, derived from lidar data, in tsunami inundation modeling by incorporating these objects as topographic highs in a finite-difference scheme solving nonlinear long wave equations. This incorporated model yielded tsunami characteristics on land that differ from those in the conventional DEM model. We propose that 3D shapes of buildings and structures should be investigated in more detail for tsunami hazard assessments in urban areas. For example, we treated them as intact solid bodies in our calculation, but after the 2011 Tohoku earthquake, many coastal buildings were destroyed by the tsunami. How do we account for destruction of buildings and the loss of their effectiveness as a barrier in tsunami modeling? The spatial resolution we applied, which was $2/9$ arcsec (about 5 m) in the finest grid, is still too coarse to represent narrow alleys in residential districts, which may result in underestimating tsunami inundation areas because these small tsunami corridors are erased in the interpolation process used to make the incorporated model. A more desirable spatial resolution, at a meter scale or finer, would impose severe computational demands. Because the tsunami flow around buildings is likely to be very complicated, it may be better to apply the governing equations with a high degree of accuracy rather than rely on two-dimensional nonlinear shallow water theory. We are investigating these issues using the very large dataset from the 2011 Tohoku earthquake for mitigation of future tsunami damage.

Acknowledgments Dr. Hong Kie Thio, Dr. Phil Cummins, and Dr. David Burbidge kindly provided us with the URSGA tsunami code. We also thank the editor, Vicente Santiago-Fandiño and an anonymous reviewer. Some Figures were made using Generic Mapping Tools (Wessel and Smith 1998) and ArcGIS.

References

- Ammon CJ, Lay T, Kanamori H, Cleveland M (2011) A rupture model of the 2011 off the Pacific coast of Tohoku earthquake. *Earth Planets Space* 63:693–696
- British Oceanographic Data Centre, GEBCO (General Bathymetric Chart of the Oceans) (2010) http://www.gebco.net/data_and_products/gridded_bathymetry_data
- DeMets C, Gordon RG, Argus DF (2010) Geologically current plate motions. *Geophys J Int* 181:1–80
- Geospatial Information Authority of Japan (2011) Tsunami inundation map of the 2011 Tohoku-oki earthquake on a scale of 1 to 100000 (in Japanese). <http://www.gsi.go.jp/kikaku/kikaku60003.html>
- Imamura F, Koshimura S, Murashima Y, Akita Y, Nitta Y (2011) Implementation of the tsunami simulation for the 2011 Tohoku earthquake (in Japanese). http://www.tsunami.civil.tohoku.ac.jp/hokusai3/J/events/tohoku_2011/model/dcrc_ver1.1_111107.pdf
- Ito T, Ozawa K, Watanabe T, Sagiya T (2011) Slip distribution of the 2011 off the Pacific coast of Tohoku earthquake inferred from geodetic data. *Earth Planets Space* 63:627–630
- Jakeman JD, Nielsen OM, VanPutten K, Mleczko R, Burbidge D, Horspool N (2010) Towards spatially distributed quantitative assessment of tsunami inundation models. *Ocean Dyn* 60:1115. doi:10.1007/s10236-010-0312-4
- Kido Y, Fujiwara T, Sasaki T, Kinoshita M, Kodaira S, Sano M, Ichiyama Y, Hanafusa Y, Tsuboi S (2011) Bathymetric feature around Japan Trench obtained by JAMSTEC multi narrow beam survey, MIS036-P58 (in Japanese). Japan Geoscience Union Meeting, 2011
- Ministry of Land, Infrastructure, Transport and Tourism (2006) Segmentalized land utilization data. <http://nlftp.mlit.go.jp/ksj/jpgis/datalist/KsjTmplt-L03-b.html>
- National Police Agency (2012) Damage caused by the 2011 off the Tohoku Pacific coast earthquake (in Japanese). <http://www.npa.go.jp/archive/keibi/biki/higaijyokyo.pdf>
- Okada Y (1985) Surface deformation due to shear and tensile faults in a half-space. *Bull Seismol Soc Am* 75:1135–1154
- Satake K (2002) Tsunamis. In: Lee WHK, Kanamori H, Jennings PC, Kisslinger C (eds) *International handbook of earthquake and engineering seismology*, vol 81A. Academic, Amsterdam, pp 437–451
- Satake K, Fujii Y, Harada T, Namegaya Y (2013) Time and space distribution of coseismic slip of the 2011 Tohoku earthquake as inferred from tsunami waveform data. *Bull Seismol Soc Am* 103:1473, accepted
- Suito H, Nishimura T, Tobita M, Imakiire T, Ozawa S (2011) Interplate fault slip along the Japan Trench before the occurrence of the 2011 off the Pacific coast of Tohoku earthquake as inferred from GPS data. *Earth Planets Space* 63:615–619
- Tohoku Tsunami Joint Survey Group (2011) The 2011 off the Pacific coast of Tohoku earthquake tsunami information. <http://www.coastal.jp/tsunami2011>
- Wessel P, Smith WHF (1998) New, improved version of generic mapping tools released. *EOS Trans Am Geophys Union* 79:579
- Yagi Y, Fukahata Y (2011) Rupture process of the 2011 Tohoku-oki earthquake and absolute elastic strain release. *Geophys Res Lett* 38(19):L19307. doi:10.1029/2011GL048701